

Turbulent Simulation Analysis Methods

Brett Friedman¹

Troy Carter¹, Maxim Umansky²

¹UCLA Department of Physics and Astronomy, ²LLNL

Summary

- Dynamical systems theory, bifurcation theory, and chaos theory along with general analysis techniques from the field of hydrodynamics are useful in the field of plasma fluid analysis.
- Plasma turbulence is either low or high dimensional chaos. If it is low dimensional, phase space orbits can be reconstructed from a single experimental or simulation time signal. Permutation entropy analysis is one way to test the dimensionality and to inform the construction of the phase space orbits.
- Proper Orthogonal Decomposition (POD) uses full spatio-temporal simulation data to establish the most important modes of a dynamical system. It can be used to determine the effective dimensionality of turbulence.
- If plasma turbulence is high dimensional chaos, many modes are involved. Mode-decomposed energy dynamics analysis that uses the equations and spatial information from simulations can determine which modes inject energy, which dissipate it, and which act passively. Different choices of basis functions including Fourier modes, linear eigenmodes, and POD modes can be used in the analysis.

Method of Time Delays: Reconstructing the Phase Space Trajectories with Experimental Measurements

Dynamical System: $\mathbf{X}_{k+1} = \mathcal{F}(\mathbf{X}_k), \quad k = 0, 1, 2, \dots$

Experimental measurement projection: $W_k = \mathcal{W}(\mathbf{X}_k)$

Under the mapping \mathcal{F} :

$$W_0 = \mathcal{W}(\mathbf{X}_0), \quad W_1 = \mathcal{W}(\mathcal{F}(\mathbf{X}_0)), \quad W_2 = \mathcal{W}(\mathcal{F}(\mathcal{F}(\mathbf{X}_0))), \quad \dots$$

\mathbf{X}_0 can be specified by a series of projected measurements:

$$\mathbf{X}_0 = \{W_0, W_1, \dots, W_{d_e-1}\}, \quad \mathbf{X}_k = \{W_k, W_{k+1}, \dots, W_{k+d_e-1}\}$$

Any set of measurements can specify \mathbf{X}_k

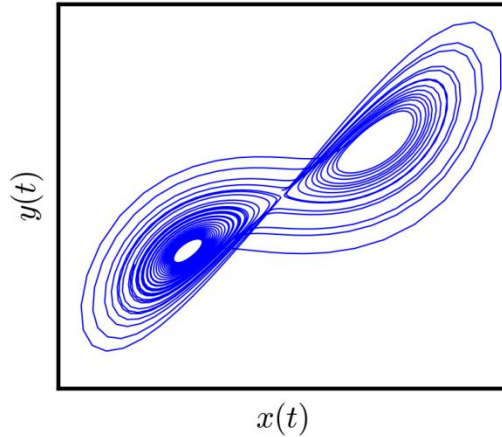
$$\mathbf{X}_k = \{W_k, W_{k+\tau}, \dots, W_{k+(d_e-1)\tau}\}$$

$\tau =$ subsampling time, $d_e =$ embedding dimension $\geq 2d_f + 1$

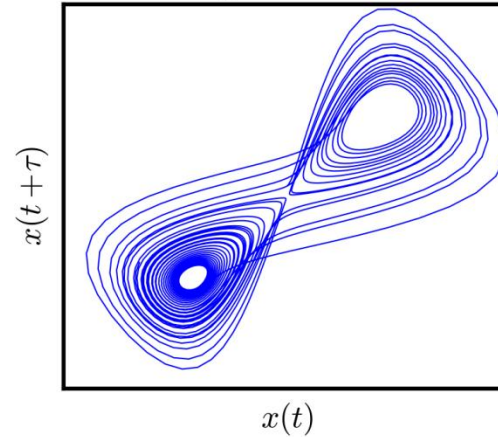
Time Delay Smoothly Reconstructs Phase Space Orbits

Lorenz Model: $\dot{x} = 10(x - y)$ $\dot{y} = x(28 - z) - y$ $\dot{z} = xy - \frac{8}{3}z$

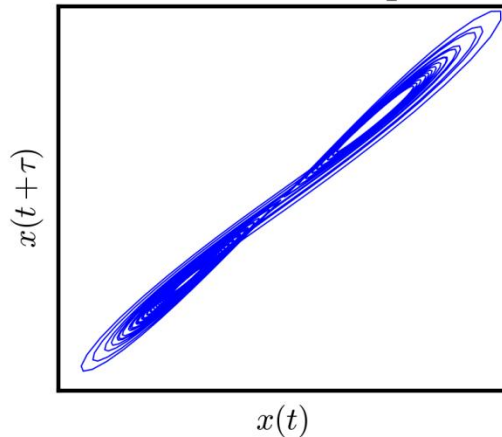
Lorenz Attractor



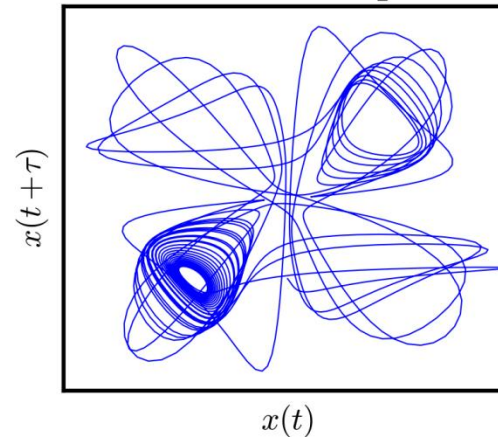
Time Delay Reconstruction



Under Subsampled



Over Subsampled



Permutation Entropy: A Measure of the Complexity of Time Signals and the Dimension of an Attractor

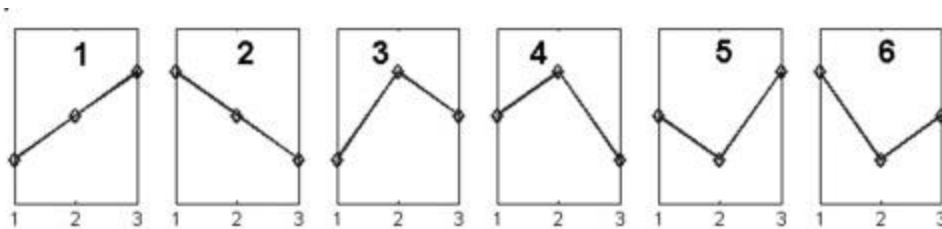
Begin with time delay reconstructed vectors:

$$\mathbf{X}_k = \{W_k, W_{k+\tau}, \dots, W_{k+(n-1)\tau}\}, \quad k = 0, 1, \dots, N$$

Rank the components in each vector.

For example, $\{9, 3, 5\} \rightarrow \{3, 1, 2\}$

There are $N = n!$ possible permutations

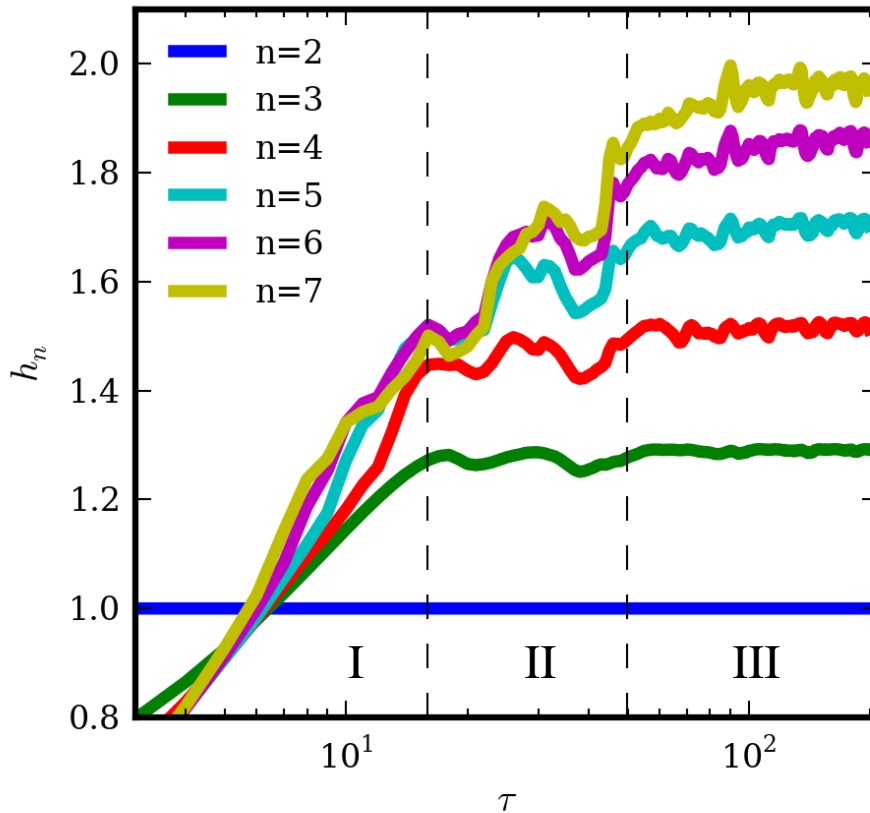


Determine the probability p_j for each permutation, then, the permutation entropy is $P_n = -\sum_{j=1}^N (p_j \log_2 p_j)$

Normalizations: $h_n = P_n / \log_2(n - 1)$

$$H_n = P_n / \log_2(N), \quad 0 \leq H_n \leq 1$$

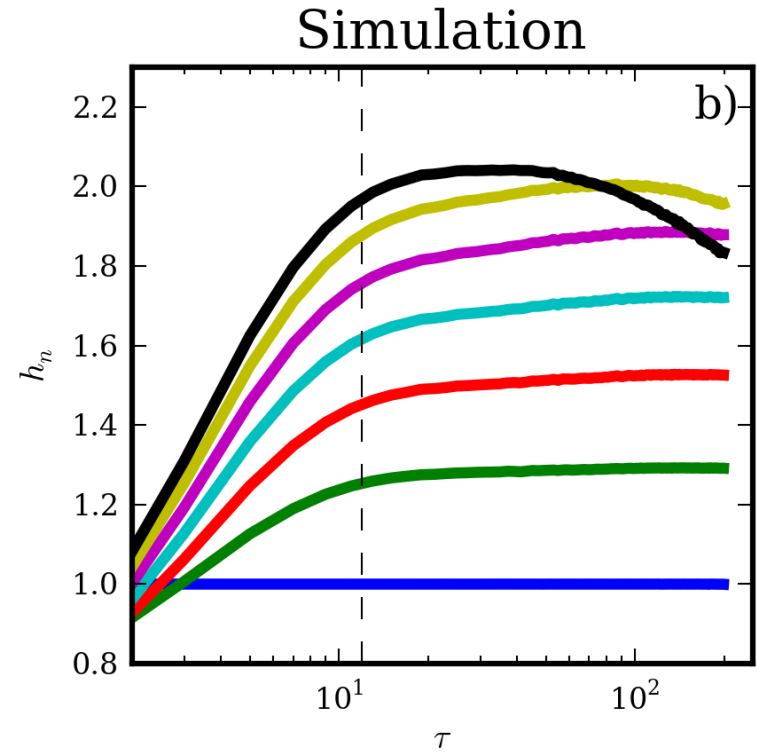
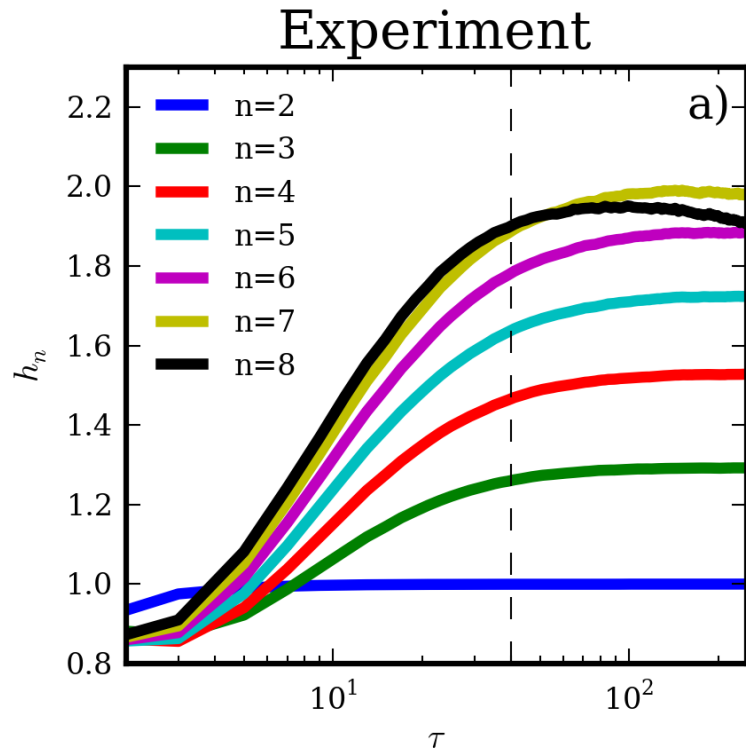
Choosing the Optimal Subsampling Time and Embedding Dimension



- I. Redundancy Effect - points are too highly correlated
- II. Saturation - points become less correlated
- III. Irrelevance Effect - every point is uncorrelated from every other point

- The optimal subsampling time is the first dashed line separating regions I and II.
- The optimal embedding dimension (n) has maximum entropy at the first dashed line

LAPD Attractor Embedding Dimension Too High for Permutation Entropy Analysis

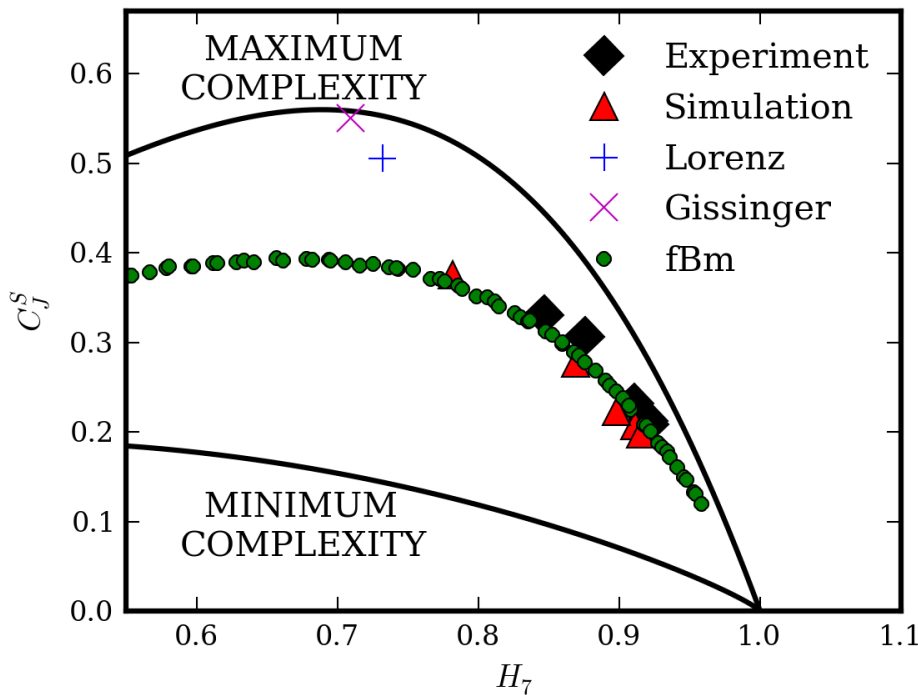


- Total time places a practical limit on the maximum embedding dimension. Need enough reconstructed vectors to fill out the probability distribution.
- Permutation entropy and time delay reconstruction are limited to low-dimensional chaos

The Location of the Data in the Entropy-Complexity Plane is More Robust to Embedding Dimension than Entropy Alone

$$C_{SJ} = -2 \frac{P_n \left(\frac{p+p_e}{2} \right) - \frac{1}{2} P_n(p) - \frac{1}{2} P_n(p_e)}{\frac{N+1}{N} \log_2(N+1) - 2 \log_2(2N) + \log_2(N)} H_n(p)$$

p_e is the probability distribution with maximum entropy: $p_j = 1/N$



- Complexity is an information measure. It quantifies the amount of repetitive structure in a time signal
- Lorenz and Gissinger are low-dimensional chaotic models
- Fractional Brownian motion (fBm) is a stochastic model with high complexity
- Chaotic and stochastic models occupy different places in the C-H plane

The Proper Orthogonal Decomposition (POD)

The energetically weighted data is put into matrix form and decomposed by Singular Value Decomposition

$$A(\vec{r}_i, t_j) = \sum_{q=1}^{N_{\text{POD}}} \sigma_q u_q(\vec{r}_i) w_q(t_j)$$

Both spatial and temporal vectors are orthogonal:

$$\sum_i u_q(\vec{r}_i) u_l(\vec{r}_i) = \sum_j w_q(t_j) w_l(t_j) = \delta_{ql}$$

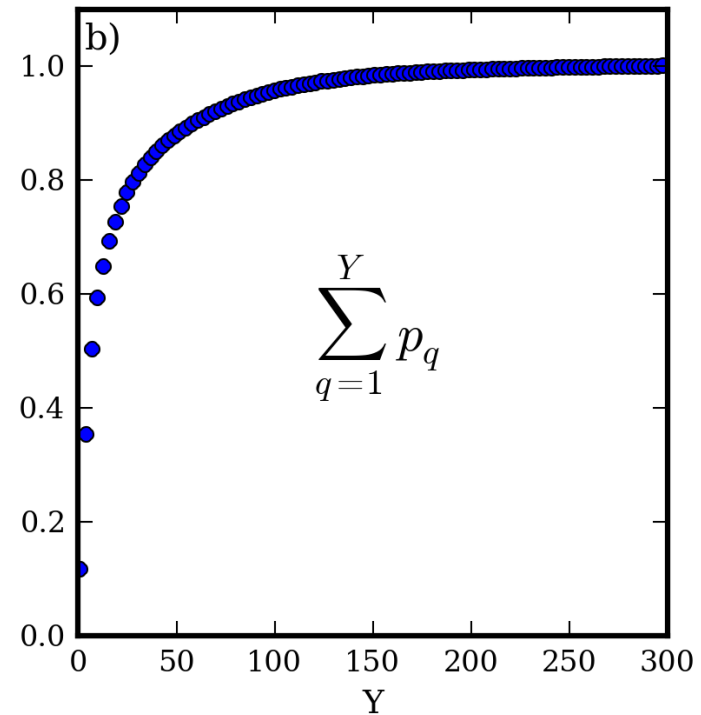
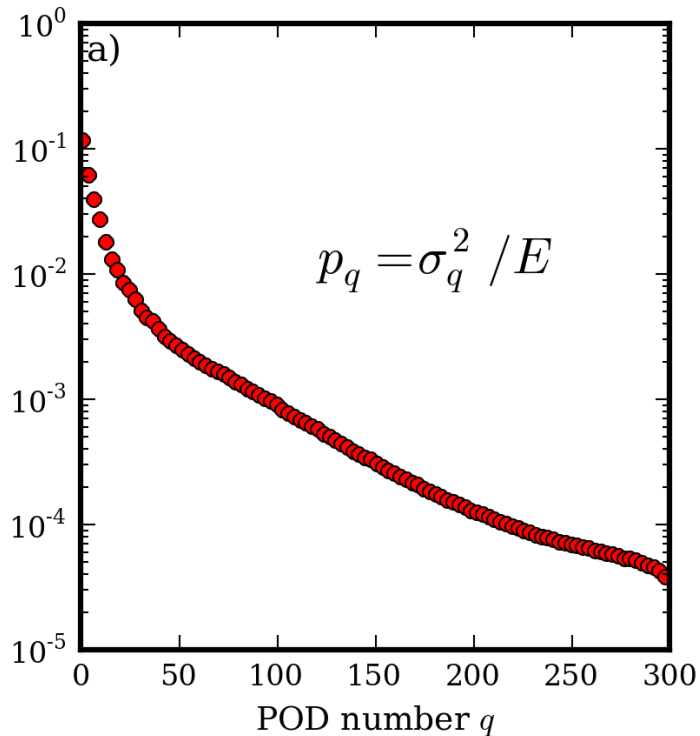
$$E = \sum_{i,j} A_{ij}^2 = \sum_q \sigma_q^2, \quad E_q = \sigma_q^2$$

The POD is an optimal decomposition in that for the rank h truncation

$$A_{ij}^{(h)} = \sum_{q=1}^h \sigma_q u_q(\vec{r}_i) w_q(t_j)$$

$$\|A - A^{(h)}\|^2 = \min \{ \|A - B\|^2 \}, \text{ for } \text{rank}(B) = h$$

The POD Entropy Measures the Stochasticity of the Data



$$\text{Entropy: } H_q = - \sum_{q=1}^{N_{\text{POD}}} p_q \log(p_q) / \log(N_{\text{POD}}) = 0.67$$

- Fast POD decay indicates fewer important modes. Gives low entropy.
- First 58 POD modes constitute 90% of the LAPD turbulent energy. Too many for low-dimensional chaos

Fourier-Decomposed Energy Dynamics

The continuity equation

$$\frac{\partial N}{\partial t} = -\mathbf{v}_E \cdot \nabla N_0 - N_0 \nabla_{\parallel} v_{\parallel e} + \mu_N \nabla_{\perp}^2 N + \{\phi, N\}$$

Potential energy of density fluctuations: $\frac{1}{2} P_0 (N/N_0)^2 = \frac{1}{2} \frac{T_0}{N_0} N^2$

Fourier decompose the fluctuations (only in parallel and poloidal directions):

$$N(\vec{r}, t) = \sum_{m,n} n_{\vec{k}}(\vec{r}, t) e^{im\theta + ik_{\parallel} z}, \quad \vec{k} = (m, n), \quad k_{\parallel} = \frac{2\pi n}{L_{\parallel}}$$

$$\begin{aligned} \sum_{\vec{k}} \frac{\partial n_{\vec{k}}}{\partial t} e^{im\theta + ik_{\parallel} z} &= \sum_{\vec{k}} \left[-\frac{im}{r} \partial_r N_0 \phi_{\vec{k}} - ik_{\parallel} N_0 v_{\vec{k}} + \mu_N \nabla_{\perp}^2 n_{\vec{k}} \right] e^{im\theta + ik_{\parallel} z} \\ &+ \frac{1}{r} \sum_{\vec{k}, \vec{k}'} \left(im n_{\vec{k}} \partial_r \phi_{\vec{k}'} - im' \partial_r n_{\vec{k}} \phi_{\vec{k}'} \right) e^{i(m+m')\theta + i(k_{\parallel} + k'_{\parallel})z} \end{aligned}$$

Multiply through by $\frac{T_0}{N_0} n_{\vec{k}'}^* e^{-im'\theta - ik'_{\parallel} z}$ and integrate over space

$$\begin{aligned} \frac{1}{2} \left\langle \frac{T_0}{N_0} \frac{\partial |n_{\vec{k}}|^2}{\partial t} \right\rangle &= \left\langle -\frac{T_0}{N_0} \frac{im}{r} \partial_r N_0 \phi_{\vec{k}} n_{\vec{k}}^* - ik_{\parallel} T_0 v_{\vec{k}} n_{\vec{k}}^* + \frac{T_0}{N_0} \mu_N \nabla_{\perp}^2 n_{\vec{k}} n_{\vec{k}}^* \right\rangle \\ &+ \left\langle \frac{T_0}{r N_0} \sum_{\vec{k}'} \left(im' n_{\vec{k}'} \partial_r \phi_{\vec{k} - \vec{k}'} n_{\vec{k}}^* - i(m - m') \partial_r n_{\vec{k}'} \phi_{\vec{k} - \vec{k}'} n_{\vec{k}}^* \right) \right\rangle \end{aligned}$$

Each Term has Meaning – Turbulent Drive, Energy Transfer, or Dissipation

Dynamical Energy Equation Forms (for each field j)

$$\frac{\partial E_j(\vec{k})}{\partial t} = Q_j(\vec{k}) + C_j(\vec{k}) + D_j(\vec{k}) + \sum_{\vec{k}'} T_j(\vec{k}, \vec{k}')$$

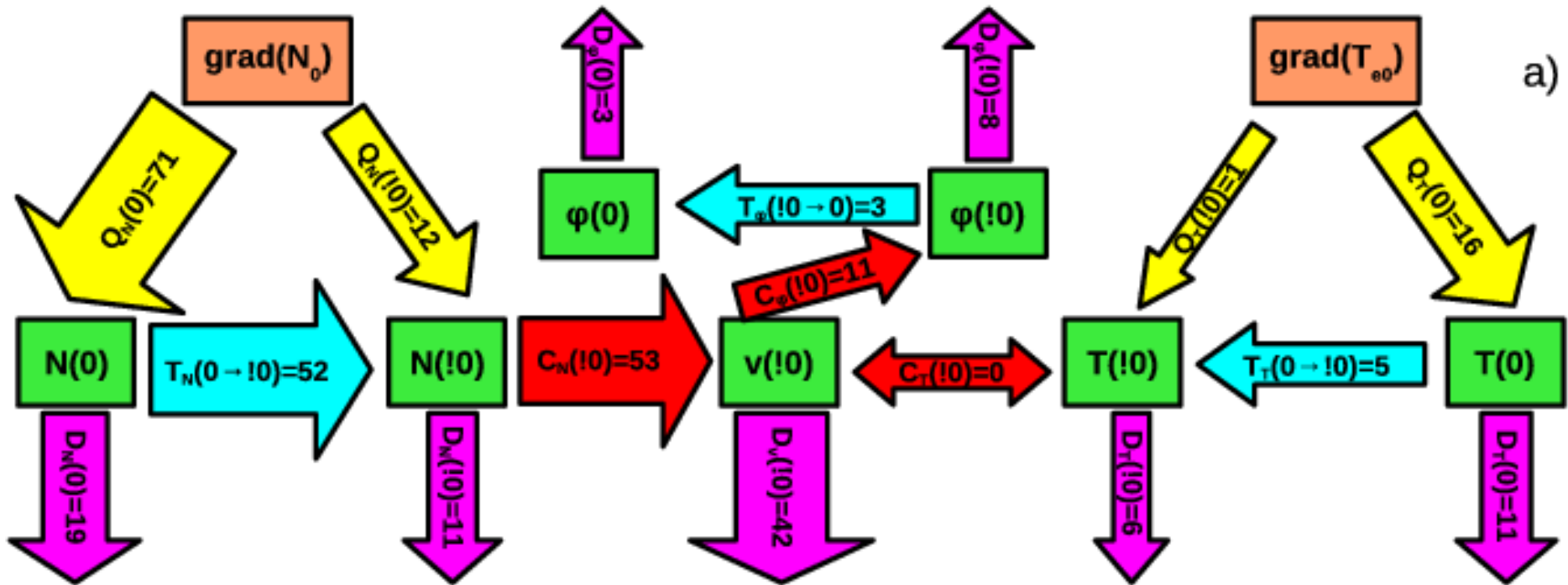
Free Energy Sources Axial compression transfer channel Dissipation Three-wave transfers

Energy Conservation Properties:

$$\sum_{k, k'} T_j(k, k') = 0, \quad \sum_j C_j(k) = 0$$

- Arakawa advection scheme conserves energy for any grid spacing
- Energy sources and dissipation do not conserve fluctuation energy – exchange energy with background gradients

Energy Dynamics Diagram Broken up Between $n=0$ and $n \neq 0$ Modes



- All summed over m
- $n=0$ separated from all $n \neq 0$, which are summed over

POD Energy Dynamics Derivation

Energy weight the data and put it into a vector, i.e. Hasegawa-Wakatani system:

$$E = \frac{1}{2} \left(\frac{T_0}{N_0} N^2 + N_0 (\nabla_{\perp} \phi)^2 \right)$$
$$A(\vec{r}, t) = \left\langle \sqrt{T_0(r)/N_0(r)} N(\vec{r}, t), \sqrt{N_0(r)} \nabla_r \phi(\vec{r}, t), \sqrt{N_0(r)} \nabla_{\theta} \phi(\vec{r}, t) \right\rangle$$

Take the SVD: $A(\vec{r}, t) = \sum_{q=1}^{N_{\text{POD}}} \sigma_q u_q(\vec{r}) w_q(t)$

Unweight the spatial data:

$$u_q(\vec{r}) = \left\langle \sqrt{T_0(r)/N_0(r)} n_q(\vec{r}), \sqrt{N_0(r)} \nabla_r \phi_q(\vec{r}), \sqrt{N_0(r)} \nabla_{\theta} \phi_q(\vec{r}) \right\rangle$$

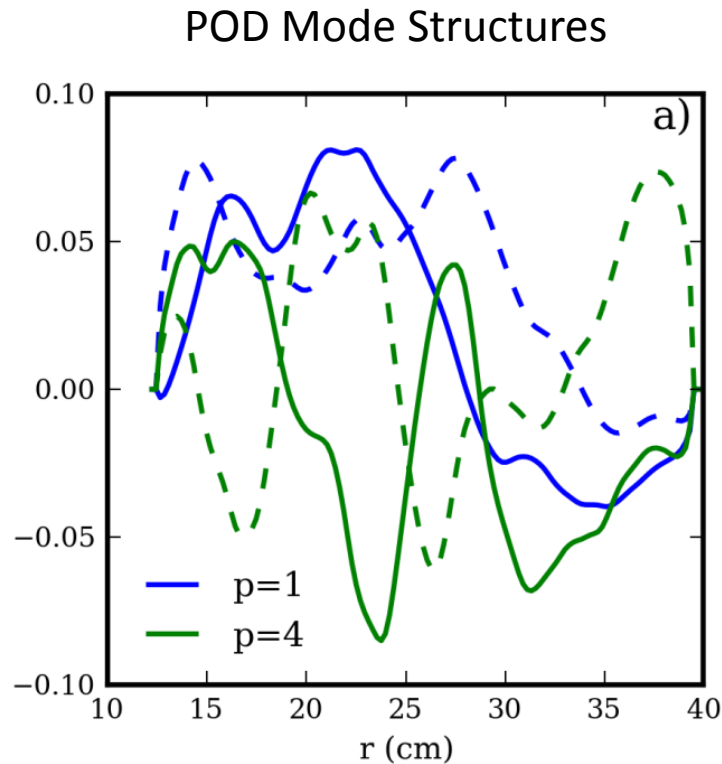
Make substitutions in equations, e.g. $N(\vec{r}, t) = \sum_{q=1}^{N_{\text{POD}}} \sigma_q n_q(\vec{r}) w_q(t)$

Multiply by e.g. $T_0/N_0 \sigma_p n_p^* w_p^*$, add equations together and volume integrate to use the POD spatial orthogonality relation.

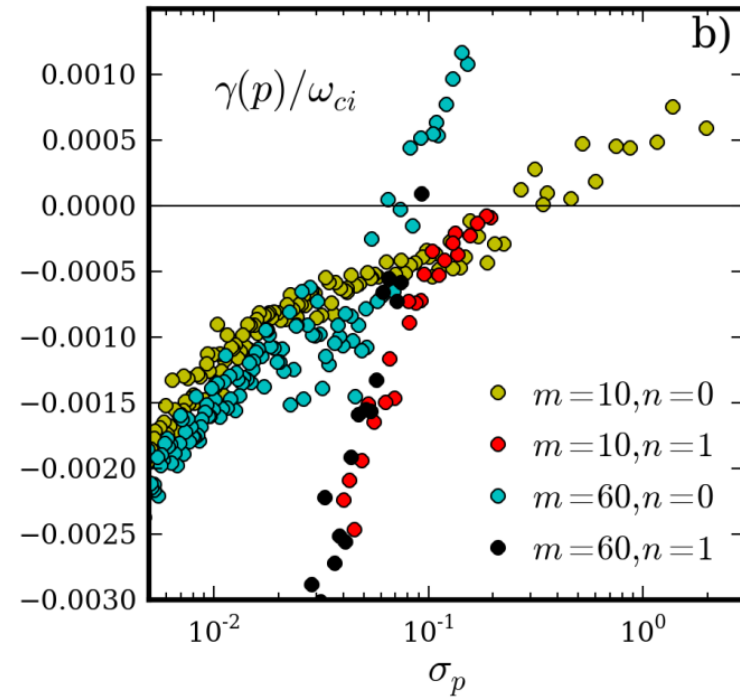
Then time integrate to use the POD temporal orthogonality relation. Result:

$$\frac{\partial E_p}{\partial t} = - \int \left(\frac{T_0}{r N_0} \sigma_p^2 n_p^* \frac{\partial \phi_p}{\partial \theta} \frac{\partial N_0}{\partial r} + \dots \right) dV$$

POD Energy Dynamics Results – POD Growth Rates



$$\gamma(p) = \left. \frac{\partial E_p}{\partial t} \right|_{lin} / \sigma_p^2$$



- Fourier-decomposed parallel-poloidal POD modes provide radial decomposition to the Fourier-decomposed energy dynamics
- Can similarly use linear eigenmodes, but more difficult due to nonorthogonality

Bibliography

1. C. Bandt and B. Pompe, "Permutation Entropy: A Natural Complexity Measure for Time Series." Phys. Rev. Lett., 88 (2002).
2. S. Futatani et al. "Spatiotemporal multiscaling analysis of impurity transport in plasma turbulence using proper orthogonal decomposition." Phys. Plasmas, 16 (2009).
3. B. Friedman et al., "Energy dynamics in a simulation of LAPD turbulence." Phys. Plasmas, 19 (2012).
4. B. Friedman et al., "Nonlinear instability in simulations of Large Plasma Device turbulence." Phys. Plasmas, 20:055704, 2013.
5. D. R. Hatch et al., "Saturation of Gyrokinetic Turbulence through Damped Eigenmodes." Phys. Rev. Lett., 106 (2011).
6. J.-H. Kim and P. W. Terry. "Energetic study of the transition to nonlinear state in two-dimensional electron temperature gradient fluid turbulence." Phys. Plasmas, 17 (2010).
7. P. Manneville, *Instabilities, Chaos and Turbulence*. Imperial College Press (2004).
8. J. E. Maggs and G. J. Morales. "Permutation entropy analysis of temperature fluctuations from a basic electron heat transport experiment." Plasma Phys. Control. Fusion, 55 (2013).
9. O. A. Rosso et al., "Distinguishing Noise from Chaos." Phys. Rev. Lett., 99 (2007).
10. M. Riedle et al., "Practical considerations of permutation entropy." Eur. Phys. J. Special Topics, 222 (2013).
11. J. Theiler, "Estimating the Fractal Dimension of Chaotic Time Series." The Lincoln Laboratory Journal, 3 (1990).